Proceedings of the 21st ICSMGE, Vienna, Austria, 14 – 19 June 2026. Pistrol, Adam & Schweiger (eds.)
Published by: ÖGG, Austrian Society for Geomechanics, Salzburg, Austria, ISBN 978-3-9503898-4-5
https://doi.org/10.53243/ICSMGE2026-1505

Pile Group Supported Bridges Under Scour Conditions: Numerical Modelling

Ansam Al-Karawi, Luke J. Prendergast, Nick Thom
University of Nottingham, Nottingham, United Kingdom, alyaa48@nottingham.ac.uk , ansam.alkarawi@gmail.com

Mo'men Ayasrah
School of Transportation and Logistics Engineering, Wuhan University of Technology, Wuhan 430063, China

ABSTRACT: Erosion poses a substantial problem for structures founded in flowing water such as bridge abutments and piers. Erosion reduces the embedment of foundations, potentially causing excessive structural deformation and tilting, ultimately compromising the stability and integrity of entire bridge structures. Such serious damage can lead to an increase in the collapse risk, with a resulting impact on human safety. Understanding how scour occurs, and reducing the resulting effect on a structure's stability, remains a considerable challenge. In this study, the impact of scour hole formation on the lateral loading behavior of a bridge pile group is examined. The implications for structural health monitoring are also explored. To this end, a Winkler spring-based numerical model is developed, and used to investigate how scour formation affects the lateral response of pile foundations under elastic conditions. Scour holes significantly influence the lateral deflection and bending moments of pile groups, and these effects become particularly pronounced when soil stress history is considered. The consideration of stress history effects provides a more realistic representation of soil-pile interaction, as it captures the changes in overburden pressure and soil stiffness resulting from scour-induced stress reductions.

KEYWORDS: Scour hole shape, bridges, numerical modelling, pile group foundations.

1 INTRODUCTION

Bridges serve as essential infrastructure elements, vital for both public transportation and global trade (Hamidifar et al., 2022; Fagundes et al., 2024). Consequently, their failure results in substantial economic impacts and severe disruptions to society (Hamidifar et al., 2022; De Falco & Mele, 2002). For example, in the U.S., the annual expense for repairing flood-related damage to bridges on federally supported major highways is around $50 million (Lagasse et al., 2007; Shinoda et al., 2008). Since the financial consequences of bridge collapse can exceed the original construction costs significantly, mitigating flood-related risks is critical (Arneson et al., 2012). Although bridges are indispensable, they remain highly susceptible to natural disasters, with scour and flooding being the primary causes of their failure (Arneson et al., 2012; Briaud et al., 2001; Chavan, 2021; Chavan et al., 2021; Hosseini & Amini, 2015; Kazemian et al., 2023; Prendergast et al., 2016).

Scour is the gradual erosion of soil around bridge foundations—such as piers and abutments—due to water flow, weakening their structural integrity by removing supporting soil (Arneson et al., 2012; Bao et al., 2017). Total scour depths comprise three main types: long-term riverbed degradation, contraction scour near the bridge, and localized erosion around piers or abutments (Arneson et al., 2012). Chaven (2021) warned that scour-related structural failures are particularly hazardous due to their sudden occurrence generally without visible signs.

The effects of scour on pile-supported bridges are significant: scour can increase pile displacement and bending moments along the pile (Bennet et al 2009; Chavan 2021; Chortis et al., 2020). Research has shown that scour erosion changes the fundamental static and dynamic behavior of structures and can increase bending moments and displacements (Arneson et al., 2012). For single piles, the scour is typically initiated as a relatively symmetrical, often circular or inverted elliptical, cone-shaped pit due to the formation of a downflow, a horseshoe vortex, and wake vortices. However, the presence of a pile group fundamentally alters this pattern, leading to the creation of an asymmetrical scour hole shape (Chambel et al., 2024; Jiang and Lin, 2021).

Scour around pile groups is a complex phenomenon that differs significantly from scour around single piers, often resulting in an asymmetrical scour hole shape due to interference effects, jet flow, and sheltering between individual piles (Chambel et al., 2024; Jiang and Lin, 2021). However, most existing studies focus on single piles and pile groups subjected to uniform scour. Bennett et al. (2009) evaluated a pile foundation supporting Kansas Bridge 45, in terms of the lateral behavior under scoured conditions. The effects of scour depth and pile head boundary conditions on the total deflections of the pile were examined. The study isolated the pile group behavior without fully integrating the bridge superstructure's influence. They also modelled the pile group as an equivalent single pile, an approach which, though computationally efficient, may not fully capture the complex interactions between individual piles in a group under varying scour conditions. Similarly, Prendergast et al. (2016) modelled a whole bridge subjected to uniform scour but simulated the pile group as an equivalent single pile. Chen et al. (2014) also assumed uniform scour around a modelled bridge pier in their work. Several studies investigated bridge behavior under scour conditions using various analytical approaches. Klinga and Alipour (2015) performed comprehensive structural analyses including buckling assessment, longitudinal/transverse pushover evaluations, and modal examinations of scoured bridge systems. More recently, Khandel and Soliman (2021) advanced scour modeling techniques by creating a deep learning-based integrated neural network capable of assessing multiple flood hazard intensities and simulating the structural response of bridge foundations subjected to scour effects. These studies demonstrate the evolution of scour analysis methodologies from conventional structural engineering approaches to advanced computational techniques incorporating artificial intelligence in recent years.

There have been few research studies focused on the non-uniformity of scour considering 3D numerical analysis of the whole bridge and stress history of soil after scour. Fioklou and Alipour (2019) investigated the effects of non-uniform soil erosion on the dynamic characteristics and seismic performance of bridges. The study primarily examines non-uniform scour (e.g., differing scour depths at upstream vs. downstream piers) under seismic loading, which limits its applicability to bridges in regions where both floods and earthquakes are prevalent. In addition, time-dependent seismic fragility analysis is used by Guo et al. (2016) to study the performance of two scoured

bridges under seismic loads over their service life while also considering the uncertainty of scour hazard and its dependency on time. The non-uniformity of scour creates significant challenges for bridge stability.

The non-uniform scour effect on entire bridge systems, particularly in relation to 3D bridge simulations, remains a critical knowledge gap due to the lack of comprehensive studies on how non-uniform scour influences global bridge stability. This asymmetry can induce uneven foundation stiffness, torsional loads, and differential settlements, significantly altering the bridge's responses. Therefore, this study aims to develop a high-fidelity 3D numerical model in MATLAB to simulate non-uniform scour evolution around pile group foundations. The post-scour stress history effects will also be considered. MATLAB programming is used as a virtual testing ground due to the ease of use of its computational environment for matrix manipulations. It should be noted that any code-based computational environment can also be used.

2 CASE STUDY - BRIDGE MODEL

2.1 *Bridge description*

To assess the impact of asymmetric scour effects on the response of pile group foundations in semi-integral bridges, an idealized case study was conducted using an example modelled bridge under various scour scenarios. The study investigates various scour stress-history effects including reducing the overburden soil pressure according to the scour depth, as well as maintaining the original stress history (pre-scour conditions). Furthermore, the analysis is performed on medium dense sandy soil (Prendergast et al., 2016).

This study simulates a bridge featuring a concrete box-girder deck and two spans, each measuring 15 m in length, utilizing MATLAB. This bridge is considered to be exposed to water currents. The bridge deck dimensions are 30 m length, 12 m width and 1.2 m thick. There are four box girders (details are illustrated in Figure 1). The cross-section of the deck is 14.4 m^2. The bridge deck is centrally supported by an 8 m tall pier with a diameter of 1 m. The pier rests on a pile foundation consisting of four drilled shafts, each with a diameter of 0.85 m and a length of 12 m. The piles have a cross-sectional area of 0.567 m^2, a moment of inertia of 0.0256 m^4, and a torsional constant of 0.0512 m^4. The configuration of the pile group is 2 by 2, with a spacing of three times the pile diameter between each pile. The water level is 2 m below the top of the pier, creating triangular hydrodynamic pressure that decreases linearly along the pier's depth. The geometry, material properties of each bridge component, and section details, are shown in Figure 1 and Table 1, where section A-A represents the pile group configuration and section B-B illustrates the deck's box girder dimensions.

To evaluate the impact of asymmetric scour on the static response of the bridge, lateral loading-displacement (*p-y*) curves are implemented on the piles. The curves are considered linear in this preliminary analysis, and the soil is considered as a medium dense sand only, (Table 2 (Das, 1990)). The relative density of sandy soil is 50% for medium dense sand, while the soil bulk unit weight is 18.5 kN/m^3.

Table 1. Geometry and material properties of the modelled bridge

Parameter	Deck	Pier	Cap	Piles
Young's modulus, E (N/m^2)	2×10^{10}	2×10^{10}	2×10^{10}	2×10^{10}
Poisson's ratio, v	0.2	0.2	0.2	0.2
Shear modulus, G (N/m^2)	0.9×10^{10}	0.9×10^{10}	0.9×10^{10}	0.9×10^{10}
Cross section Area, A (m)	14.4	0.7854	1	0.5675
Moment of Inertia, I (m^4)	0.7280 172.8	0.0491	0.0833	0.0256
Torsional constant, J (m^4)	2.07e3	0.0982	1	0.0512

Table 2. Relative density of different soil (Das, 1990)

Density	Ø°	D_r %	N
Medium dense sand	30-36	35-65	10-30

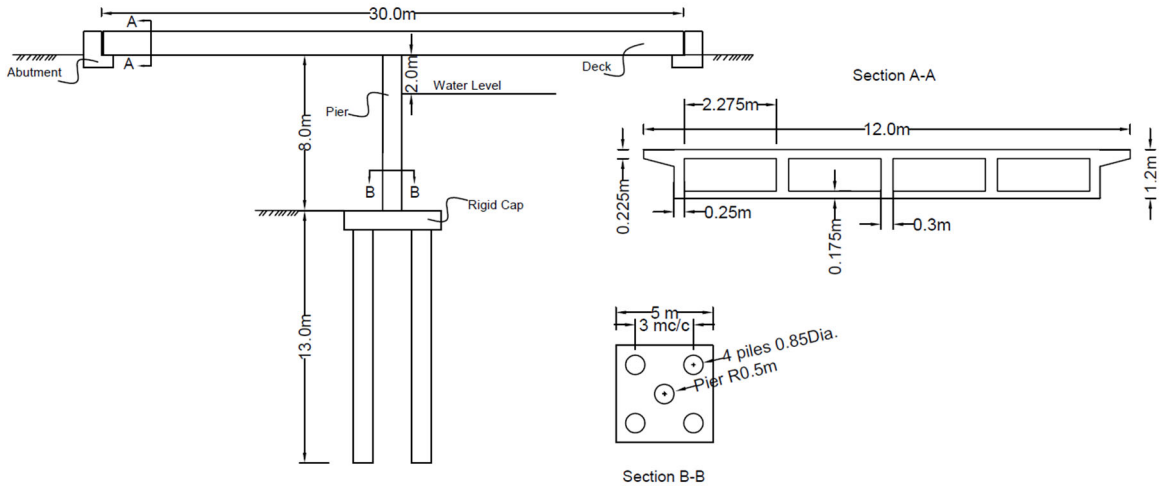

Figure 1. Bridge structure details

3 NUMERICAL MODELLING

3.1 *Structural modelling*

Numerical techniques, including the finite element method (FEM), play a crucial role in analyzing bridge structures (Fu and Wang 2015). Among these, the *p-y* method for modelling soil-structure interaction, is a useful approach for assessing bridge scour, simulating the response of laterally loaded piles through empirically derived *p-y* curves. This method is based on Winkler-foundation beam theory and employs *p-y* (lateral), *t-z* (axial), and *q-z* (end bearing) curves to model pile responses (Lin et al., 2014; Klinga & Alipour, 2015).

For the case study bridge in this paper, three-dimensional numerical simulations were performed using MATLAB, with model validation conducted in SAP2000. MATLAB, developed by The MathWorks, Inc., USA, is a powerful technical computing platform that combines computation, visualization, and programming in a user-friendly interface (Jain, 2016). Three-dimensional numerical modelling captures full 3D effects, including torsion, out-of-plane bending, and complex soil interactions, in addition to simplified simulations of the asymmetric soil loss, and localized stiffness reduction. Scour removes soil from around foundations, reducing lateral and vertical support, which can be efficiently represented in 3D by adjusting spring stiffnesses in affected zones (e.g., zero stiffness in scoured regions). Unlike 2D models—which oversimplify scour as uniform support loss—3D modeling allows for realistic scour patterns (e.g., partial pile exposure, uneven erosion depths) and better predicts bending moments, settlements, and buckling risks in piles or abutments. Additionally, dynamic scour effects (e.g., flood-induced cyclic weakening) can be modeled using time-dependent spring degradation, making 3D Winkler-based analysis critical for risk assessment and resilient bridge design.

In this study, bridge components (deck, pier, cap, and pile foundation) can be modelled using six-degree-of-freedom (DOF) Euler-Bernoulli frame elements. These elements are straight, uniform bars capable of resisting axial, bending, and torsional forces (Rao, 2010). Each element consists of two nodes, with each node having axial, transverse, and rotational DOFs totaling 12 DOFs per element (6 DOFs per node × 2 nodes). These elements form the basis for assembling the global stiffness matrices $[\mathrm{K}]_{global}$.

The bridge deck is modeled with roller supports at each end, allowing longitudinal movement while restricting displacements in all other directions. For a linear elastic 3D beam, the static equilibrium is expressed using Equation (1).

$$[\mathrm{K}]_{global}.\{d\} = \{F\} \tag{1}$$

Here, $[\mathrm{K}]_{global}, \{d\}$, and $\{F\}$ represent the global stiffness matrix, nodal displacement vector (6 DOFs per node), and applied load vector, respectively.

For 3D analysis, each node has 6 DOFs, 3 translations (u_x, u_y and u_z) and 3 rotations (θ_x, θ_y, and θ_z), then the nodal displacement vector $\{d\}$ is calculated using Equation (2)

$$\{d\} = [u_{x1}, u_{y1}, u_{z1}, \theta_{x1}, \theta_{y1}, \theta_{z1}, u_{x2}, u_{y2}, u_{z2}, \theta_{x2}, \theta_{y2}, \theta_{z2}]^T \tag{2}$$

To calculate the global matrix Equation (3), the transformation matrix $[T]$ can be used to transform local element coordinates into global structural coordinates. A planar transformation matrix $[T]$ is applied (Ferreira 2009; Sabah et al., 2022; Chandrasekaran 2018):

$$[K]_{global} = [K]_{local}.[\mathrm{T}]'.[\mathrm{T}] \tag{3}$$

$$[T] = \begin{bmatrix} t & 0 & 0 & 0 \\ 0 & t & 0 & 0 \\ 0 & 0 & t & 0 \\ 0 & 0 & 0 & t \end{bmatrix} \tag{4}$$

$$\mathrm{t} = \begin{bmatrix} C_{Xx} & C_{Yx} & C_{Zx} \\ C_{Xy} & C_{Yy} & C_{Zy} \\ C_{Xz} & C_{Yz} & C_{Zz} \end{bmatrix} \tag{5}$$

$$C_{Xx} = \cos\theta X_X \tag{6}$$

Here, θX_x, θY_x and $\theta Z_x$are the angles between global axes (X, Y, Z) and the local x-axis.

The local stiffness matrix $[K]_{local}$ incorporates axial (K_{axial}), Equation (7), torsional ($K_{tortional}$), Equation (8), and flexural (in z and y directions) stiffness ($K_{flexural\_z/y}$) components, Equation (9):

$$K_{axial} = \frac{EA}{L}\begin{bmatrix} 1 & -1 \\ -1 & 1 \end{bmatrix} \tag{7}$$

$$K_{tortional} = \frac{GJ}{L}\begin{bmatrix} 1 & -1 \\ -1 & 1 \end{bmatrix} \tag{8}$$

$$K_{flexural_{z\,or\,y}} = \frac{EI_{zory}}{L^3}\begin{bmatrix} 12 & 6L & -12 & 6L \\ 6L & 4L^2 & -6L & 2L^2 \\ -12 & -6L & 12 & -6L \\ 6L & 2L^2 & -6L & 4L^2 \end{bmatrix} \tag{9}$$

3.2 *Soil – structure interaction*

Soil-structure interaction (SSI) is a critical aspect in the design and analysis of structures, particularly bridge foundations exposed to environmental factors like scour (Bao, et al., 2017; Fioklou & Alipour 2019; Hazzar et al., 2022; Klinga and Alipour, 2015; Prendergast, et al., 2016). In this study, the bridge pile elements are discretized into 1 m segments as shown in Figure 2. Two horizontal springs are assigned along the embedded pile depth to represent the soil reaction in longitudinal and transverse directions. As outlined in Section 1, scour reduces soil stiffness. Consequently, in this study, the spring values at each embedded pile point are adjusted based on the scour depth, considering two cases of overburden stress distribution along the pile depth (Case 1 and Case 2)

Case 1: After scouring, the vertical stress distribution along the pile shifts, beginning from the new riverbed level, (considering the scour effect).

Case 2: The vertical stress distribution remains the same as in the no-scour condition, except that the scoured soil layer is removed, (ignoring the scour effect). Figure 3(a) illustrates the spring stiffness distribution before scour for medium dense soil. Figure 3(b–d) depict the spring distribution along the pile for scour depths of 1D, 2D, and 3D (where D is the pile diameter) across the soil type and for both cases.

To determine the modulus of subgrade reaction (K) (MN/m²), the following steps are taken:

- First, the small-strain shear modulus (G_0) is computed using the cone penetration test (CPT) profile along the pile length (Lunne and Christopherson 1983) (Equation 10).
- Next, the elastic Young's modulus (E_0) is calculated with depth using Equation (12).

- Finally, the soil stiffness (k_s) (MN/m) is derived using Equation (14), by multiplying the value of subgrade reaction at each spring depth by the distance between two points (a).

It should be noted that, for simplicity, the soil is considered elastic at the small-strain value for the simulations in this study.

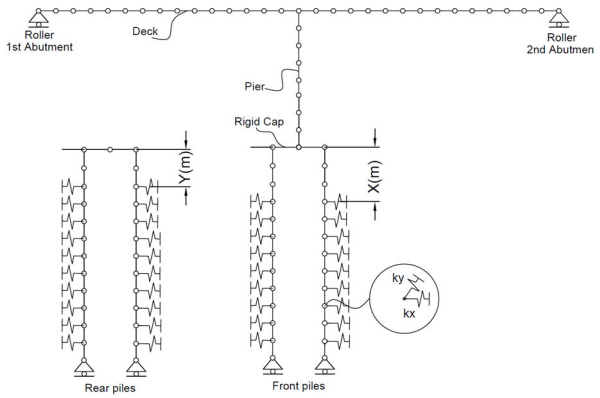

Figure 2. Schematic diagram of whole bridge model

$$q_c = 60\ (\sigma'_v)^{0.7}.\exp\ (2.91\ Dr) \tag{10}$$

$$G_O = q_c[A + B\eta - C\eta^2]^{-1} \tag{11}$$

$$E_o = 2\ G_o(1 + \nu) \tag{12}$$

$$K = \frac{1.0\ E_O}{(1-\nu^2)}\left[\frac{E_O D^4}{E_P I_P}\right]^{\frac{1}{12}} \tag{13}$$

$$k_S = K\ .\ a \tag{14}$$

Where:
σ'_v = vertically effective stress (kPa)
Dr = relative density (%)
ν = Poisson's ratio
E_o= small strain Young's modulus of soil (kPa)
D = pile diameter (m)
$E_P I_P$ = flexural rigidity (N.m^2)
A= 0.0203, B=0.00125, C=1.216e-6, $\eta = q_c(P_a\sigma'_v)^{-0.5}$
P_a = 100 kPa

3.3 *Scour Modelling*

In this research, scour effects are simulated by eliminating Winkler springs at the specified scour depth to replicate asymmetrical erosion patterns. For general scour conditions, springs are uniformly removed (set to zero stiffness) from the same depth across the foundation. However, to better represent real-world conditions, the model accounts for differential erosion between upstream and downstream piles in a pile group. Since upstream piles are more exposed to water flow, they experience deeper scour compared to sheltered downstream piles. Therefore, the selected scour depths in this study reflect these realistic environmental conditions, with detailed scenarios presented in Table 3.

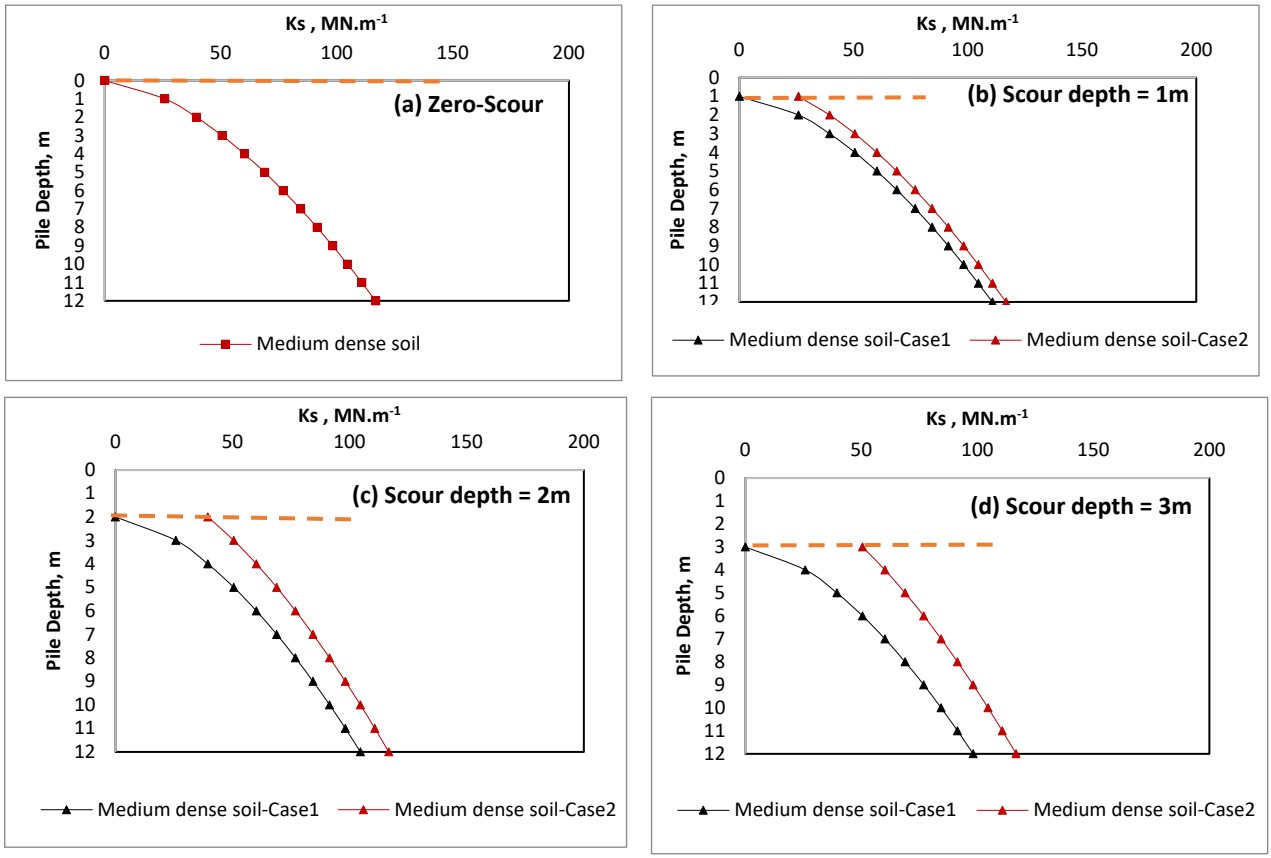

Figure 3. Soil stiffness profile for different scour depths; a) zero scour, b) 1 m, c) 2 m, and d) 3 m.

Table 3. Scour depth variations in this study

Test No.	*Front Pile Scour Depth, X (m)*	*Rear Pile Scour Depth Y(m)*
1	*0*	*0*
2	*1*	*1*
3	*2*	*2*
4	*3*	*3*
5	*2*	*1*
6	*3*	*1*
7	*3*	*2*

3.4 *Loading*

In general, bridges are subjected to various static and dynamic loads, including vehicle traffic, wind, and water currents. The accumulation of debris at the upstream or downstream ends of a bridge, as well as underneath it, can modify the bridge's geotechnical and hydraulic behavior. Given that many bridges span narrow streams, the presence of debris may have a greater influence on their performance (Khan, 2010). In this study, two kinds of loading were applied on the bridge structure, wind and debris loading, with the load being off center, i.e. causing rotation. All the equations to calculate the wind loads (at the top of the pier) and debris loads (at a point 2 m from pier end) are stated in Lin et al., (2015). Scour exposure lowers the bed level, increasing the effective area subjected to flow forces, and thus can result in hydrodynamic loads on bridge foundations. In the current study, a simplified lateral load that remains unchanged across all scour scenarios, is applied, and the effect of scour depth on the load magnitude is neglected in the analysis for simplicity.

4 ANALYSIS AND RESULTS

The study investigates the impact of different scour scenarios—including uniform (Tests 2–4) and non-uniform (Tests 5–7) scour depths (see Table 3) - on the response of a bridge supported by a pile group. Two overburden stress distribution cases in medium dense sandy soil were considered: Case 1, where post-scour overburden stress and stiffness profile were reduced by subtracting the scour depth from the total stress distribution, and Case 2, where they remained unchanged. The analysis focused on the effects of scouring on lateral deflection (u_x) and bending moment in the y-direction, providing insights into how varying scour conditions influence pile group behavior under different soil stress conditions.

4.1 *Lateral deflection responses*

Figure 4 presents the lateral response of piles under various scour depth conditions. As depicted in Figure 4(a,b), the lateral deflection of both front and rear piles increases with scour depth in uniform scour scenarios (Tests 2–4). Notably, the front piles exhibit greater deflection compared to the rear piles in all non-uniform scour cases, which is expected as there is deeper scour depth at the front piles than at the rear piles for these cases. The findings show that lateral deflections are greater in Case 1 (where overburden stress is adjusted after scouring) compared to Case 2 (where overburden stress remains constant), for both front and rear piles under uniform and non-uniform scour conditions. This difference occurs because Case 2 maintains soil stiffness despite scour-induced stress relief. Therefore, the study suggests that future analyses should account for the stress history effect caused by scour, as previous stress conditions may influence soil behavior and pile response. This consideration could lead to more accurate predictions of scour-induced deformations.

4.2 *Bending moment of pile group*

Scour-induced loss of lateral soil support around pile groups amplifies structural responses to loads and modifies bending moment distributions, with the response varying significantly between uniform (equal around all piles) and non-uniform (variable depth) scour conditions. As shown in Figure 5(a) and (b) (Tests 2-4), the rigid pile cap ensures identical bending moments in front and rear piles under uniform scour. However, in Test 6 (non-uniform scour), the front pile deflection approaches that of a 3 m uniform scour scenario. The analysis also reveals that Case 1 yields greater moments than Case 2, mirroring the lateral deflection trends, emphasizing the need to account for stress history effects in post-scour soil-pile interaction assessment.

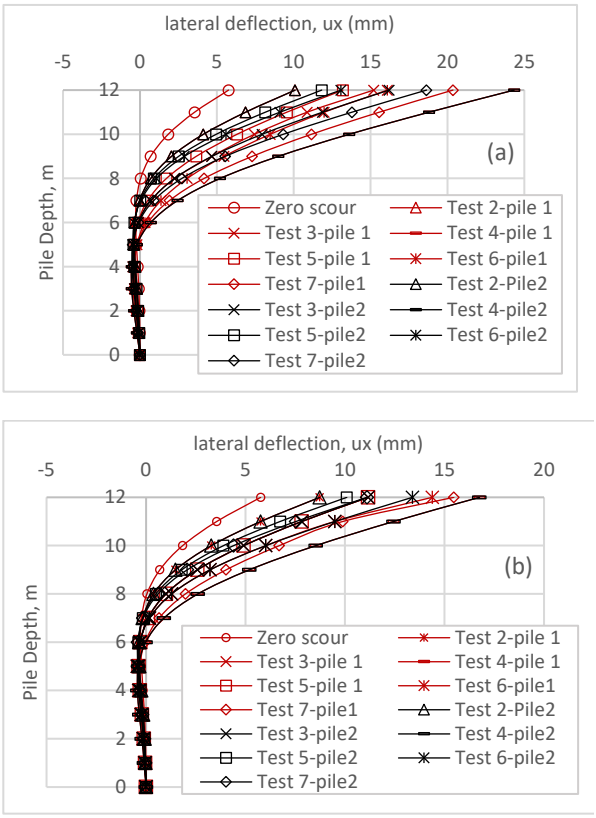

Figure 4. Lateral pile deflection profile responses of front and rear piles (a) Case 1 and (b) Case2.

5 CONCLUSIONS

The evaluation of scour depth effects on pile group response is crucial for assessing the structural integrity of bridges supported by pile foundations. As scour progresses over time, it reduces soil support around the foundation, leading to increased lateral deflections and bending moments in the piles. Both deflection and moment magnitudes grow with greater scour depths, with front piles experiencing more significant effects than rear piles in non-uniform scour conditions due to their greater exposure to erosion. Three-dimensional scour modeling proves particularly valuable for capturing realistic pile group behavior, especially when considering the whole bridge modelling and considering that front piles typically undergo more severe scouring than rear piles because of flow-pile interactions. The study concludes that both uniform and non-uniform scouring significantly influence pile responses, and it strongly recommends accounting for stress history changes following scouring events in structural assessments.

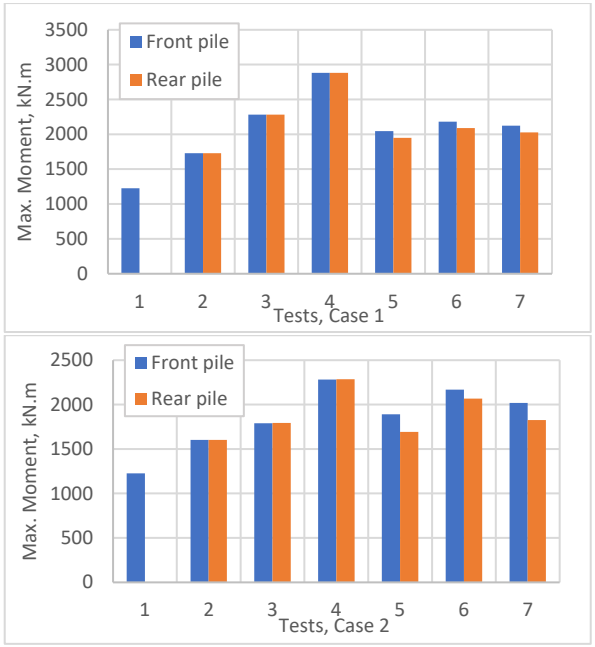

Figure 5. Maximum moment for different tests and a) Case 1, b) Cas.

6 ACKNOWLEDGEMENTS

The author (Ansam Al-Karawi) gratefully acknowledges the contribution of Schlumberger Foundation which awarded the author with a fellowship supporting her PhD study through Faculty for the Future Program.

7 REFERENCES

Arneson, L.A., Zevenbergen, L.W., Lagasse, P.F. and Clopper, P.E., 2012. Evaluating scour at bridges (No. FHWA-HIF-12-003). National Highway Institute (US).

Bao, T., Swartz, R.A., Vitton, S., Sun, Y., Zhang, C. and Liu, Z., 2017. Critical insights for advanced bridge scour detection using the natural frequency. Journal of Sound and Vibration, 386, pp.116-133.

Bennett, C.R., Lin, C., Parsons, R. and Han, J., 2009. Evaluation of behavior of a laterally loaded bridge pile group under scour conditions. In Structures Congress 2009: Don't Mess with Structural Engineers: Expanding Our Role (pp. 1-10).

Briaud, J.L., Ting, F.C.K., Chen, H.C., Cao, Y., Han, S.W. and Kwak, K.W., 2001. Erosion function apparatus for scour rate predictions. Journal of geotechnical and geoenvironmental engineering, 127(2), pp.105-113.

Chambel, J., Fazeres-Ferradosa, T., Miranda, F., Bento, A.M., Taveira-Pinto, F. and Lomonaco, P., 2024. A comprehensive review on scour and scour protections for complex bottom-fixed offshore and marine renewable energy foundations. Ocean Engineering, 304, p.117829.

Chandrasekaran, S., 2018. Advanced Structural Analysis with MATLAB®. CRC Press.

Chavan, V.S., 2021. Finite Element Modeling of a Pier-on-Bank Bridge Scour (Doctoral dissertation, The University of North Carolina at Charlotte).

Chavan, V.S., Chen, S.E., Shanmugam, N.S., Tang, W., Diemer, J., Allan, C., Braxtan, N., Shukla, T., Chen, T. and Slocum, Z., 2021. An analysis of local and combined (global) scours on piers-on-bank bridges. CivilEng, 3(1), pp.1-20.

Chen, C.C., Wu, W.H., Shih, F. and Wang, S.W., 2014. Scour evaluation for foundation of a cable-stayed bridge based on ambient vibration measurements of superstructure. Ndt & E International, 66, pp.16-27.

Chortis, G., Askarinejad, A., Prendergast, L.J., Li, Q. and Gavin, K., 2020. Influence of scour depth and type on p–y curves for monopiles in sand under monotonic lateral loading in a geotechnical centrifuge. Ocean Engineering, 197, p.106838.

Das, B.M., 2019. Advanced soil mechanics. CRC press.

De Falco, F. and Mele, R., 2002. The monitoring of bridges for scour by sonar and sedimetri. NDT & E International, 35(2), pp.117-123.

Fagundes, D.F., Pimpão, C.Y. and Servi, S.P., 2024. Mechanical behaviour of dredging waste in the port of Rio Grande by adding stabilizing agents. International Journal of Geotechnical Engineering, 18(4), pp.433-443.

Ferreira, A.J., 2009. MATLAB codes for finite element analysis: solids and structures. Dordrecht: Springer Netherlands.

Fioklou, A. and Alipour, A., 2019. Significance of non-uniform scour on the seismic performance of bridges. Structure and Infrastructure Engineering, 15(6), pp.822-836.

Fu, C.C. and Wang, S., 2014. Computational analysis and design of bridge structures. CRC Press.

Guo, X., Wu, Y. and Guo, Y., 2016. Time-dependent seismic fragility analysis of bridge systems under scour hazard and earthquake loads. Engineering Structures, 121, pp.52-60.

Hamidifar, H., Mohammad Ali Nezhadian, D. and Carnacina, I., 2022. Experimental study of debris-induced scour around a slotted bridge pier. Acta Geophysica, 70(5), pp.2325-2339.

Hazzar, L., Karray, M. and Pasic, A., 2022. Simplified approach for soil-spring stiffness prediction of pile group. International Journal of Geotechnical Engineering, 16(4), pp.415-425.

Hosseini, R. and Amini, A., 2015. Scour depth estimation methods around pile groups. KSCE Journal of Civil Engineering, 19(7), pp.2144-2156.

Jain, A.K., 2016. Dynamics of structures with MATLAB® applications. Pearson Education India.

Jiang, W. and Lin, C., 2021. Scour effects on vertical effective stresses and lateral responses of pile groups in sands. Ocean Engineering, 229, p.109017.

Kazemian, A., Yee, T., Oguzmert, M., Amirgholy, M., Yang, J. and Goff, D., 2023. A review of bridge scour monitoring techniques and developments in vibration-based scour monitoring for bridge foundations. Advances in Bridge Engineering, 4(1), p.2.

Khan, M.A., 2010. Bridge and highway structure rehabilitation and repair.

Khandel, O. and Soliman, M., 2021. Integrated framework for assessment of time-variant flood fragility of bridges using deep learning neural networks. Journal of Infrastructure Systems, 27(1), p.04020045.

Klinga, J.V. and Alipour, A., 2015. Assessment of structural integrity of bridges under extreme scour conditions. Engineering Structures, 82, pp.55-71.

Lagasse, P. F., Clopper, P. E., Zevenbergen, L. W., and Girard, L. W., "Countermeasures to protect bridge piers from scour", NCHRP Report 593, Washington DC, 2007.

Lin, C., Bennett, C., Han, J. and Parsons, R., 2015. Effect of soil stress history on scour evaluation of pile-supported bridges. Journal of Performance of Constructed Facilities, 29(6), p.04014178.

Lin, C., Han, J., Bennett, C. and Parsons, R.L., 2014. Case history analysis of bridge failures due to scour. In Climatic effects on pavement and geotechnical infrastructure (pp. 204-216).

Lunne, T., Christopherson, H.P., 1983. Interpretation of cone penetrometer data for offshore sands. In: Proceedings of the Offshore Technology Conference OTC4464. Houston, Texas.

Prendergast, L.J., Hester, D. and Gavin, K., 2016. Determining the presence of scour around bridge foundations using vehicle-induced vibrations. Journal of Bridge Engineering, 21(10), p.04016065.

Prendergast, L.J., Hester, D., Gavin, K. and O'sullivan, J.J., 2013. An investigation of the changes in the natural frequency of a pile affected by scour. Journal of sound and vibration, 332(25), pp.6685-6702.

Rao, S.S., 2010. The finite element method in engineering. Elsevier.

Sabah, R., Öztorun, N.K. and Sayin, B., 2022. Development of an FEA program with full-size stiffness and mass matrices for dynamic analysis of high-rise buildings: A comparison with SAP2000. Case Studies in Construction Materials, 17, p.e01490.

Shinoda, M., Haya, H. and Murata, S., 2008, November. Nondestructive evaluation of railway bridge substructures by percussion test. In Fourth Int Conf Scour Eros (pp. 285-290).